

# Synthesis and Separation of the Enantiomers of the Neuropeptide S Receptor Antagonist (9R/S)-3-Oxo-1,1-diphenyl-tetrahydro-oxazolo[3,4-*a*]pyrazine-7-carboxylic Acid 4-Fluoro-benzylamide (SHA 68)

Claudio Trapella,<sup>†,‡</sup> Michela Pela,<sup>†,‡</sup> Luisa Del Zoppo,<sup>†</sup> Girolamo Calo,<sup>‡</sup> Valeria Camarda,<sup>‡</sup> Chiara Ruzza,<sup>‡</sup> Alberto Cavazzini,<sup>§</sup> Valentina Costa,<sup>§</sup> Valerio Bertolasi,<sup>§,||</sup> Rainer K. Reinscheid,<sup>⊥</sup> Severo Salvadori,<sup>†</sup> and Remo Guerrini<sup>\*,†</sup>

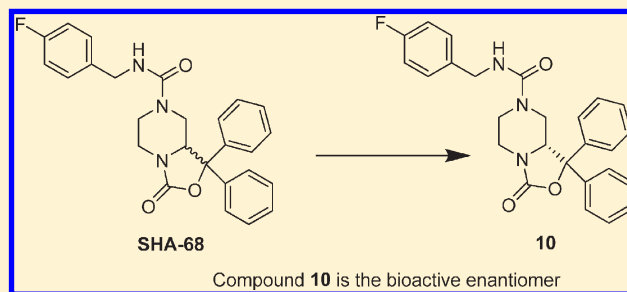
<sup>†</sup>Department of Pharmaceutical Sciences and Biotechnology Center and <sup>‡</sup>Department of Experimental and Clinical Medicine, Section of Pharmacology and Neuroscience Center, and National Institute of Neuroscience, University of Ferrara, via Fossato di Mortara 19, 44100 Ferrara, Italy

<sup>§</sup>Department of Chemistry and <sup>||</sup>Centre for Structural Diffractionometry, University of Ferrara, via L. Borsari 46, 44100 Ferrara, Italy

<sup>⊥</sup>Department of Pharmaceutical Sciences, University of California Irvine, 2214 Natural Sciences I, Irvine, California 92697, United States

**S** Supporting Information

**ABSTRACT:** This study reports the synthesis, chromatographic separation, and pharmacological evaluation of the two enantiomers of the neuropeptide S receptor (NPSR) antagonist (9R/S)-3-oxo-1,1-diphenyl-tetrahydro-oxazolo[3,4-*a*]pyrazine-7-carboxylic acid 4-fluoro-benzylamide (SHA 68). The (9R)-3-oxo-1,1-diphenyl-tetrahydro-oxazolo[3,4-*a*]pyrazine-7-carboxylic acid 4-fluoro-benzylamide (compound **10**) and (9S)-3-oxo-1,1-diphenyl-tetrahydro-oxazolo[3,4-*a*]pyrazine-7-carboxylic acid 4-fluoro-benzylamide (compound **10a**) were synthesized and their purity assessed by chiral chromatography. The absolute configuration of the enantiomer **10** has been assigned from the crystal structure of the corresponding (*S*)-phenyl ethyl amine derivative **8**. Calcium mobilization studies performed on cells expressing the recombinant NPSR demonstrated that compound **10** is the active enantiomer while the contribution of **10a** to the NPSR antagonist properties of the racemic mixture is negligible.



## INTRODUCTION

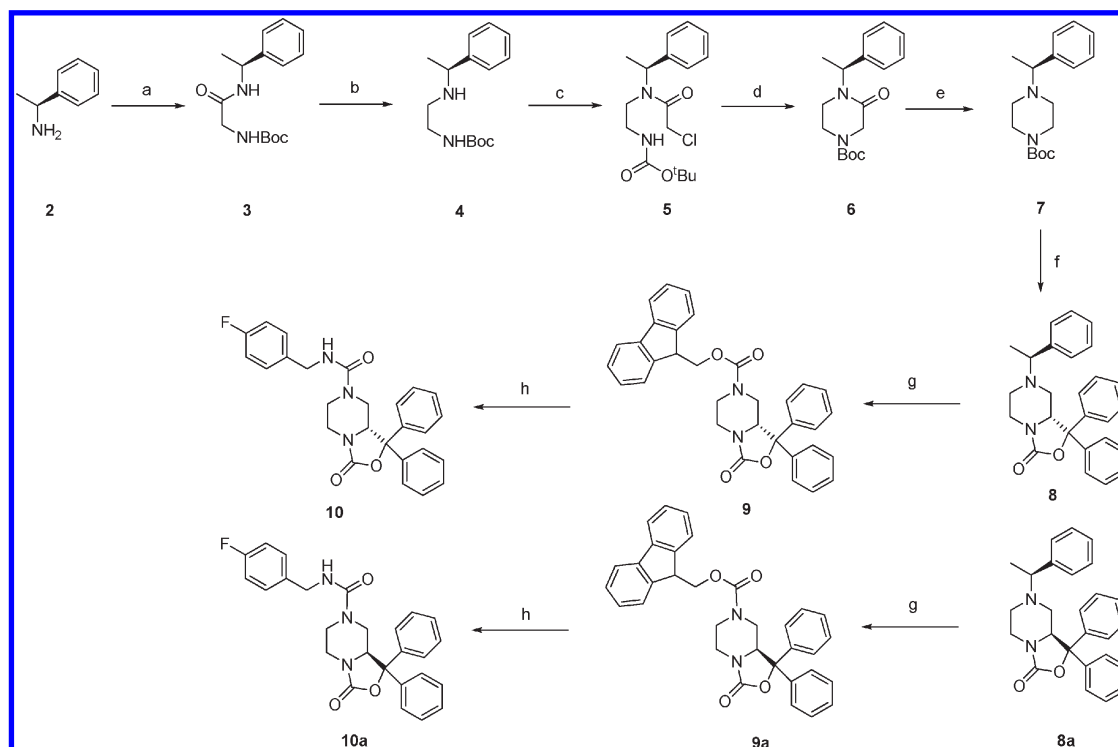
Neuropeptide S (NPS) is the last neuropeptide identified via the reverse pharmacology approach.<sup>1</sup> NPS selectively binds and activates a previously orphan GPCR receptor now referred to as NPSR.<sup>1</sup> NPSR is widely distributed in the brain, while the expression of the NPS peptide precursor is limited to few discrete brain areas.<sup>1,2</sup> The supraspinal administration of NPS in rodents produces a rather unique pattern of actions: stimulation of wakefulness associated with anxiolytic-like effects.<sup>1</sup> In addition, NPS has been reported to inhibit food intake, facilitate memory, elicit antinociceptive effects, and recent evidence suggests an involvement of the NPS/NPSR system in drug addiction (see for a review<sup>3</sup>).

Potent and NPSR selective antagonists are now required for understanding the biological functions controlled by the NPS/NPSR system. As far as peptide antagonists are concerned, these molecules were recently discovered by replacing Gly<sup>5</sup> in the natural peptide sequence with a D-amino acid. Examples of such compounds are [D-Cys(<sup>t</sup>Bu)<sup>5</sup>]NPS,<sup>4</sup> [D-Val<sup>5</sup>]NPS,<sup>5</sup> and more recently [<sup>t</sup>Bu-D-Gly<sup>5</sup>]NPS.<sup>6</sup> The first example of nonpeptide

molecules able to interact with the NPSR was reported in the patent literature by Takeda researchers.<sup>7</sup> Among the different molecules described in the patent, the compound (9R/S)-3-oxo-1,1-diphenyl-tetrahydro-oxazolo[3,4-*a*]pyrazine-7-carboxylic acid 4-fluoro-benzylamide (SHA 68; compound **1**) has been pharmacologically characterized. In vitro, compound **1** behaves as a selective, potent ( $pA_2 \cong 8$ ), and competitive antagonist at human<sup>8</sup> and murine<sup>9</sup> NPSR. In vivo, compound **1** has been reported to prevent the arousal promoting and anxiolytic-like effects elicited by NPS in mice and rats.<sup>8,9</sup> In addition, compound **1** reversed the protective effect of NPS on the NMDA receptor antagonist MK-801-induced neurotoxicity in rats.<sup>10</sup> Finally, recent findings indicate that in the rat intracerebroventricular injection of NPS increased conditioned reinstatement of cocaine seeking, whereas peripheral administration of compound **1** reduced it.<sup>11</sup> These pharmacological investigations were performed using the racemic compound **1**. Molecular modeling

**Received:** December 7, 2010

**Published:** April 05, 2011

Scheme 1. Synthesis of Compounds 10 and 10a<sup>a</sup>

<sup>a</sup> Reagents and conditions: (a) CH<sub>2</sub>Cl<sub>2</sub>, WSC, Boc-Gly-OH, room temp, 12 h; (b) LiAlH<sub>4</sub>, THF, 0 °C, 1 h; (c) chloroacetyl-chloride, EtOAc, NaHCO<sub>3</sub>, 0 °C to room temp, 24 h; (d) THF/DMF 1/1, NaH, 0 °C to room temp, 24 h; (e) THF, LiAlH<sub>4</sub>, room temp, 4 h; (f) THF, benzophenone, *sec*-BuLi, TMEDA, -78 °C to -30 °C to room temp, 24 h; (g) CH<sub>3</sub>CN, Fmoc-Cl, reflux, 12 h; (h) THF, DBU, *p*-fluoro-benzylisocyanate, room temp, 12 h.

studies investigated nonpeptide ligand binding to NPSR.<sup>12</sup> In the frame of these studies, docking analyses were performed and a defined NPSR binding pocket was proposed; of note, only the (*S*) enantiomer of compound 1 was used in such simulations. The importance of ligand chirality for NPSR interaction has been recently supported by the identification of two novel classes of nonpeptide NPSR antagonists: the quinoline<sup>13</sup> and the tricyclic imidazole<sup>14</sup> based compounds. In both cases, a single bioactive enantiomer was obtained by chiral chromatography separation from the corresponding racemic mixture.

In the present study, we report the synthesis, chiral HPLC analysis, X-ray crystallographic assignment, and *in vitro* pharmacological evaluation of the two compound 1 enantiomers.

## RESULTS AND DISCUSSION

The reference compound 1 was synthesized following the procedures reported by Okamura et al.<sup>8</sup> In Scheme 1 is described the synthetic approach adopted for the synthesis of 10 and 10a starting from (*S*)-phenyl ethyl amine. As reported in literature,<sup>15,16</sup> the use of phenyl ethyl amine was expected to induce the stereochemistry of C9 of the tetrahydro-oxazolo-[3,4-*a*]pyrazine nucleus. Unfortunately, we obtained only a slight chiral induction corresponding approximately to a 60/40% ratio determined by NMR spectroscopy. Similar results were obtained using (*R*)-phenyl ethyl amine as chiral auxiliary. Nevertheless, diastereomers 8 and 8a were successfully separated in good yield by flash chromatography. The removal of the chiral auxiliary to obtain 9 and 9a and the acylation of N7 with *p*-fluoro-benzylisocyanate to obtain final compounds were achieved using the

procedure reported by Okamura et al.<sup>8</sup> The purity grade and enantiomeric excess of 10 and 10a were determined by chiral HPLC analysis. The top panel of Figure 1 shows the chromatogram for the single enantiomer 10a (first eluted component), and the middle panel that of 10 (second eluted species) and the bottom panel of the figure displays the chromatogram for the racemate. As is evident from this figure, there is no trace of 10 in the chromatogram corresponding to the elution of 10a, nor of 10a in that of 10. To define the absolute configuration of the C9 chiral center, we explored different crystallization conditions for compounds 8, 8a, 9, 9a, and for the final products. Only with compound 8 were we able to obtain crystals suitable for further X-ray investigation. In particular, compound 8 was crystallized from ethanol/ethyl acetate, and its X-ray analysis demonstrated the absolute configuration *R* at the chiral center C9. The absolute C9 configuration of compound 8 has been assigned by reference to the unchanged chiral center C10 in configuration *S* (Figure 2). On the basis of the absolute configuration of 8, we were able to assign the absolute C9 configuration to compounds 8a, 9, 9a, and to the final products 10 and 10a.

In parallel, we performed a series of NMR experiments. In Figure 3, the enlarged [<sup>1</sup>H]NMR spectra of the C9 proton region of the 10a and 10 isomers are depicted. The coupling constant analysis between H<sub>x</sub> and H<sub>a</sub>/H<sub>b</sub> C8 protons are very similar (11.3/3.7 Hz for 10a, Figure 3A and 11.2/3.7 Hz for 10, Figure 3B) in both compounds. This result, together with X-ray data of 8 (see Figure 2), confirms the axial position of C9 proton in both enantiomers.

Next, we evaluated and compared the *in vitro* NPSR antagonist properties of compounds 1, 10, and . The three samples were

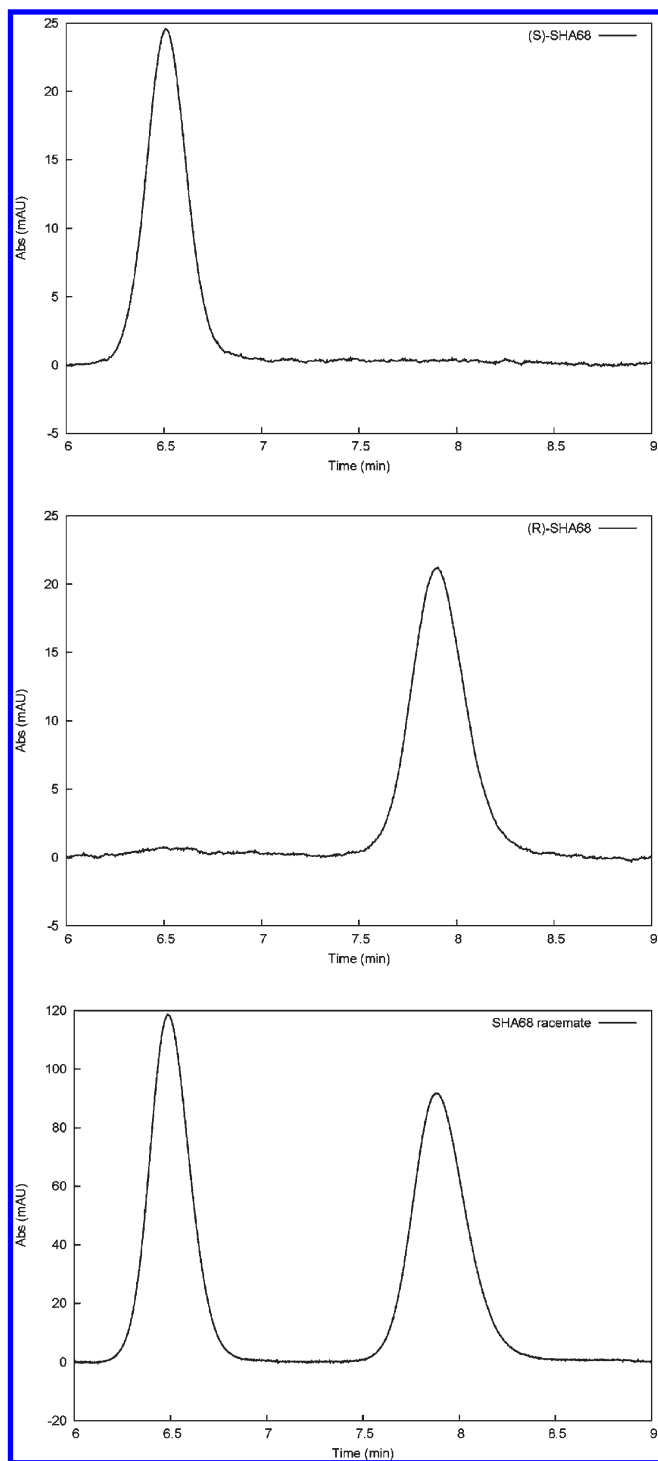


**Figure 1.** Chromatograms of compound 10a (top panel) and 10 (middle panel) in comparison with the racemate (bottom panel).

tested in calcium mobilization studies performed on HEK293 cells expressing the murine NPSR or the two isoforms of the human receptor (hNPSRAsn107 and hNPSRIle107).<sup>17</sup>

The natural peptide NPS was able to induce calcium mobilization in a concentration dependent manner in HEK 293 mNPSR ( $pEC_{50}$   $8.97 \pm 0.11$ ;  $E_{max}$   $250 \pm 11\%$ ), hNPSRAsn107 ( $pEC_{50}$ :  $9.07 \pm 0.11$ ;  $E_{max}$   $316 \pm 13\%$ ), and hNPSRIle107 ( $pEC_{50}$ :  $9.17 \pm 0.15$ ;  $E_{max}$   $333 \pm 17\%$ ). The three samples were

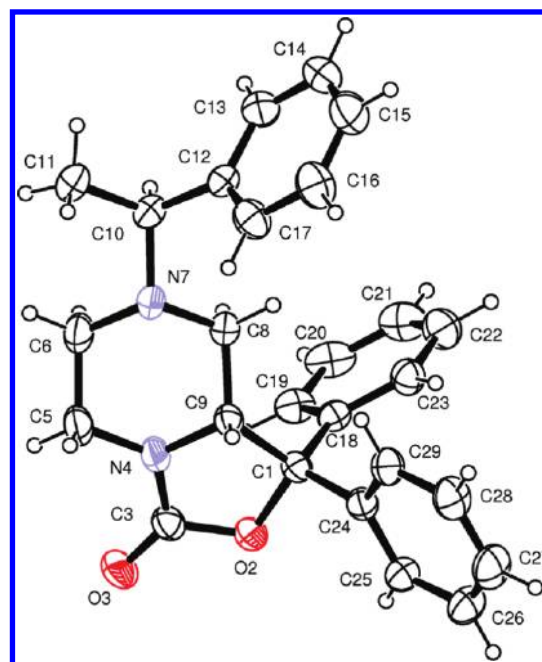


**Figure 2.** ORTEP view of compound 8. The thermal ellipsoids are drawn at 30% probability level.

challenged against the stimulatory effect of 10 nM NPS in inhibition response curves (Figure 4). Compounds 1, 10, and 10a did not stimulate per se calcium mobilization up to 10  $\mu$ M. Compound 1 inhibited in a concentration dependent manner the stimulatory effect of NPS showing similar high values of potency ( $pK_B \approx 8$ ). These values of potency are superimposable to those previously published.<sup>8,9</sup> Compound 10 was also able to antagonize in a concentration dependent manner the stimulatory effect of NPS displaying values of potency similar or slightly higher than the racemic mixture. By contrast, compound 10a showed a slight inhibitory effect only at micromolar concentrations. The values of potency of the three compounds in the three cells lines are summarized in Table 1. Collectively, these results demonstrated that compound 10 is the active enantiomer while the contribution of compound 10a to the biological activity of the racemic mixture is negligible. This information can be extremely useful for the refinement of the recently proposed molecular models of NPSR and its binding pocket.<sup>12</sup> As already mentioned in the Introduction, the relevance of ligand chirality for NPSR binding is also corroborated by the fact that the biological activity of chemically different molecules, such as the quinoline<sup>13</sup> and the tricyclic imidazole<sup>14</sup> compounds, could be attributed to a single bioactive enantiomer.

## CONCLUSION

In conclusion, the present study described the synthesis and separation of the two compound 1 enantiomers. The synthetic scheme we used can be easily scaled up to multigrams. Compound 10 was demonstrated to be the bioactive enantiomer. Nowadays, this molecule represents the standard nonpeptide NPSR antagonist that has been, and surely will be, used to investigate the biological functions controlled by the NPS/NPSR system and to evaluate the therapeutic potential of innovative drugs acting as NPSR selective ligands.

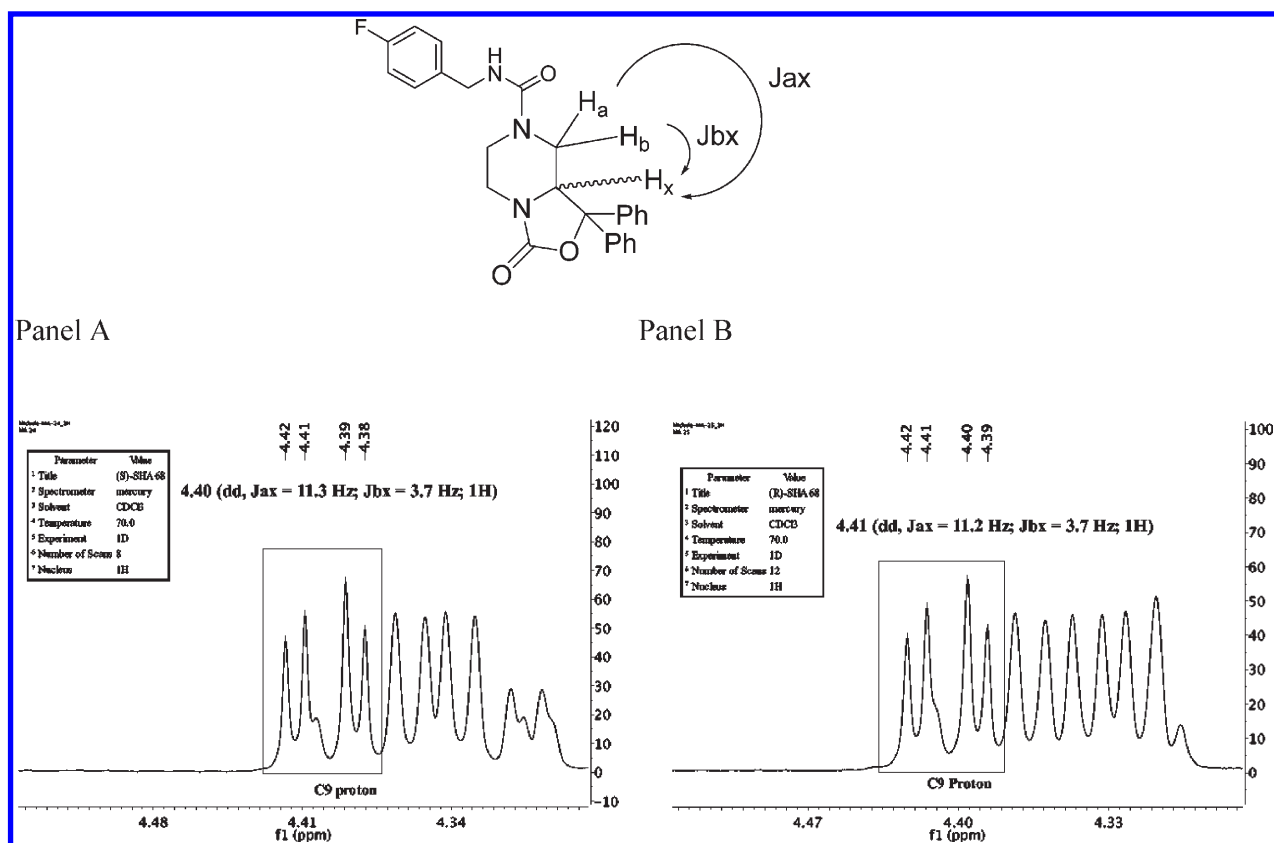


Figure 3. Enlarged  $^1\text{H}$  NMR spectra of the C9 proton region of the 10a (A) and 10 (B) isomers.

## EXPERIMENTAL SECTION

**Materials.** HPLC grade solvent were purchased from Sigma Aldrich (Steinheim, Germany). The purity of the tested compounds **1**, **10**, and **10a** has been assessed by RP-HPLC. All compounds showed >95% purity. One-dimensional and two-dimensional NMR spectra were recorded on a VARIAN 400 MHz instrument. Chemical shifts are given in ppm ( $\delta$ ) relative to TMS, and coupling constants are in Hz. MS analyses were performed on a ESI-Micromass ZMD 2000. Optical rotation data were recorded on a Perkin-Elmer polarimeter 241. Flash chromatography was carried out on a silica gel (Merck, 230–400 Mesh). Silica gel (Polygram SIL G/UV254) was used for thin layer chromatography.

### Typical Procedures for the Synthesis of 10 and 10a.

**[(1-Phenyl-ethylcarbamoyl)-methyl]-carbamic Acid tert-Butyl Ester (3).** To a stirred solution of Boc-Gly-OH (5 g, 28.5 mmol) in  $\text{CH}_2\text{Cl}_2$  (50 mL), WSC (3.64 g, 19 mmol) and (S)-phenylethyl amine (3.45 g, 28.5 mmol) were added. After 24 h at room temperature, the reaction was monitored by TLC (EtOAc/light petroleum 2:1). The organic layer was washed with 10% citric acid (20 mL), 5%  $\text{NaHCO}_3$  (20 mL), and brine (20 mL). The organic phase was dried, concentrated in vacuo, and purified by flash chromatography (EtOAc/light petroleum 2:1) to obtain **3** in 60% yield.  $^1\text{H}$  NMR (400 MHz,  $\text{CDCl}_3$ ):  $\delta$  7.31–7.24 (m, 5H, Ar), 6.62 (bs, 1H, NH-CO), 5.31 (bs, 1H, NH-Boc), 5.11 (m, 1H, CH- $\text{CH}_3$ ), 3.75 (m, 2H,  $\text{CH}_2$ -NH-Boc), 1.47 (d, 3H,  $\text{CH}_3$ -CH-Ar,  $J = 6.8$  Hz), 1.42 (s, 9H,  $^t\text{Bu}$ -).  $^{13}\text{C}$  NMR (100 MHz,  $\text{CDCl}_3$ ):  $\delta$  168.6, 156.2, 143.0, 128.7, 127.4, 126.1, 80.2, 48.7, 44.6, 28.3, 21.9. MS (ESI):  $[\text{M} + \text{H}]^+ = 279$ ;  $[\alpha]_{\text{D}}^{20} = -41$  ( $c = 0.121$  g/100 mL, chloroform).

**[2-(1-Phenyl-ethylamino)-ethyl]-carbamic Acid tert-Butyl Ester (4).** To a stirred suspension of  $\text{LiAlH}_4$  (0.85 g, 22.38 mmol) at 0 °C in

anhydrous THF, a solution of **3** (3.11 g, 11.19 mmol) was added dropwise. The reaction was monitored by TLC (EtOAc/light petroleum 3:1), and after 24 h, the excess of hydride was quenched with water and the salts were filtered through a Celite pad. The solvent was evaporated in vacuo to yield **4** (2.66 g, 10.07 mmol) in 90% yield.  $^1\text{H}$  NMR (400 MHz,  $\text{CDCl}_3$ ):  $\delta$  7.32–7.27 (m, 5H, Ar); 4.96 (bs, 1H, NH-Boc), 3.77–3.73 (q, 1H,  $\text{CH}_3$ -CH-Ar,  $J = 6.6$  Hz), 3.16–3.13 (m, 2H, NH- $\text{CH}_2$ - $\text{CH}_2$ ), 2.59–2.51 (m, 2H, NH- $\text{CH}_2$ - $\text{CH}_2$ ), 1.75 (bs, 1H, -NH), 1.42 (s, 9H,  $^t\text{Bu}$ -), 1.36–1.33 (d, 3H,  $\text{CH}_3$ -CH-Ar,  $J = 6.6$  Hz). MS (ESI):  $[\text{M} + \text{H}]^+ = 265$ ;  $[\alpha]_{\text{D}}^{20} = -29^\circ$  ( $c = 0.11$  g/100 mL, chloroform).

**{2-[(2-Chloro-acetyl)-(1-phenyl-ethyl)-amino]-ethyl}-carbamic Acid tert-Butyl Ester (5).** To a stirred solution of **4** (1.94 g, 7.34 mmol) in EtOAc (50 mL) at 0 °C, saturated solution of  $\text{NaHCO}_3$  (5 mL) was added. After 10 min, chloroacetyl chloride (1.17 mL, 14.68 mmol) was added dropwise. The reaction was monitored by TLC (EtOAc/light petroleum 3:1), and after 24 h at room temperature,  $\text{NaHCO}_3$  (2 mL) was added to the organic phase. The organic layer was separated, and the aqueous phase was extracted twice with EtOAc (50 mL). The combined organic phases were concentrate to dryness to obtain **5** in quantitative yield.  $^1\text{H}$  NMR (400 MHz,  $\text{CDCl}_3$ ):  $\delta$  7.22–6.98 (m, 5H, Ar), 5.59–5.43 (q, 1H,  $\text{CH}_3$ -CH-Ar,  $J = 8$  Hz), 4.85 (bs, 1H, NH-Boc), 4.10–3.97 (m, 2H, NH- $\text{CH}_2$ - $\text{CH}_2$ ), 3.76 (s, 2H, C=O- $\text{CH}_2$ -Cl), 3.18–3.15 (m, 2H, NH- $\text{CH}_2$ - $\text{CH}_2$ ), 1.40–1.25 (d, 3H,  $\text{CH}_3$ -CH-Ar,  $J = 8$  Hz), 1.06 (s, 9H,  $^t\text{Bu}$ ).  $^{13}\text{C}$  NMR (100 MHz,  $\text{CDCl}_3$ ):  $\delta$  170.12, 155.85, 139.47, 128.45, 128.20, 128.03, 80.69, 59.44, 42.86, 41.14, 38.24, 27.48, 19.98. MS (ESI):  $[\text{M} + \text{H}]^+ = 341$ .

**3-Oxo-4-(1-phenyl-ethyl)-piperazine-1-carboxylic Acid tert-Butyl ester (6).** To a stirred suspension of 60% NaH (1.14 g, 28.61 mmol) in a mixture of THF/DMF 1/1 (20 mL) at 0 °C, a solution of **5** (3.25 g, 9.54 mmol) in THF/DMF 1/1 (10 mL) was added. After 24 h, the



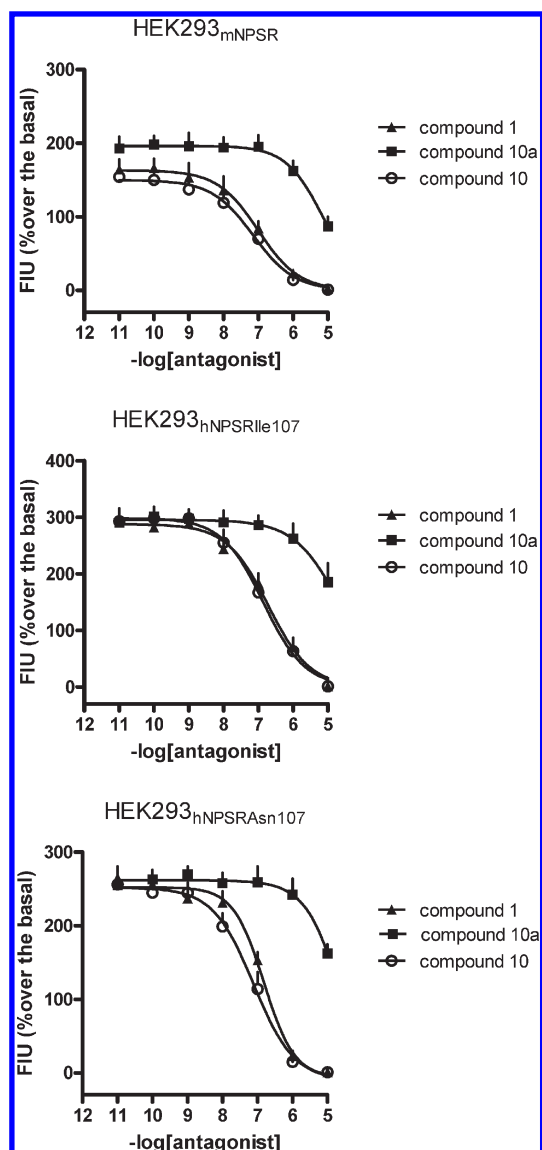


**Figure 4.** Inhibition response curves to compounds **1** (SHA 68), **10**, and **10a** in HEK293 cells expressing the murine NPSR and the human NPSR isoforms. Data are mean  $\pm$  SEM of four separate experiments made in duplicate.

**Table 1.** Potencies ( $pK_B$ ) of Compounds **1** (SHA 68), **10**, and **10a** in HEK293 Cells Expressing the Murine NPSR and the Human NPSR Isoforms

compd	mNPSR	hNPSR Ile107	hNPSR Asn107
	$pK_B$	$pK_B$	$pK_B$
<b>1</b>	8.16 (7.79–8.53)	8.03 (7.77–8.37)	7.99 (7.73–8.25)
<b>10</b>	8.29 (7.93–8.65)	8.18 (7.90–8.46)	8.28 (7.72–8.84)
<b>10a</b>	<6	<6	<6

reaction was quenched by adding  $\text{NH}_4\text{Cl}$  saturated solution (15 mL), and the solvent was removed in vacuo. The residue was dissolved in EtOAc (50 mL) and washed twice with water (20 mL). The organic layer was dried, evaporated under reduced pressure, and the crude product purified by flash chromatography (eluent: EtOAc/light petroleum 1:1) to obtain **6** in 45% yield.  $^1\text{H}$  NMR (400 MHz,  $\text{CDCl}_3$ ):

$\delta$  7.36–7.28 (m, 5H, Ar), 6.08 (q, 1H,  $\text{CH}_3\text{-CH-Ar}$ ,  $J = 8$  Hz), 4.23–4.18 (d, 1H,  $\text{N-CH}_2\text{Ha-C=O}$ ,  $J = 20$  Hz), 4.10 (d, 1H,  $\text{N-CH}_2\text{Ha-C=O}$ ,  $J = 20$  Hz), 3.62 (bs, 1H,  $\text{CH}_2$  piperazine), 3.27 (bs, 1H,  $\text{CH}_2$  piperazine), 3.19 (bs, 1H,  $\text{CH}_2$  piperazine), 2.83 (bs, 1H,  $\text{CH}_2$  piperazine), 1.53–1.51 (d, 3H,  $\text{CH}_3\text{-CH-Ar}$ ,  $J = 8$  Hz), 1.45 (s, 9H,  $^t\text{Bu-}$ ).  $^{13}\text{C}$  NMR (100 MHz,  $\text{CDCl}_3$ ):  $\delta$  165.44, 153.78, 139.41, 128.63, 127.68, 127.36, 80.69, 50.08, 47.98, 40.24, 28.32, 15.34. MS (ESI):  $[\text{M} + \text{H}]^+ = 305$ ;  $[\alpha]_{\text{D}}^{20} = -116.0^\circ$  ( $c = 0.318$  g/100 mL, chloroform).

*4-(1-Phenyl-ethyl)-piperazine-carboxylic Acid tert-Butyl Ester (7)*. To a stirred suspension of  $\text{LiAlH}_4$  (453 mg, 18.9 mmol) in anhydrous THF (20 mL) at room temperature, a solution of **6** (1.15 g, 3.78 mmol) in THF (10 mL) was added. After 30 min, the reaction was completed as showed by TLC analysis (EtOAc/light petroleum 1:2). The reaction was quenched by adding 15% NaOH (1 mL) and  $\text{Et}_2\text{O}$  (20 mL). The resulting precipitate was filtered through a Celite pad, and the solvent was concentrate to dryness. The crude product was purified by flash chromatography (eluent: EtOAc/light petroleum 1:2) to give **7** (920 mg, 3.17 mmol) in 84% yield.  $^1\text{H}$  NMR (400 MHz,  $\text{CDCl}_3$ ):  $\delta$  7.31–7.25 (m, 5H, Ar), 3.41–3.35 (m, 5H,  $\text{CH}_2\text{-N-Boc}$ ,  $\text{CH-CH}_3$ ), 2.41–2.33 (m, 4H,  $\text{CH}_2\text{-N}$ ), 1.43 (s, 9H,  $^t\text{Bu-}$ ), 1.36 (d, 3H,  $\text{CH}_3\text{-CH-Ar}$ ).  $^{13}\text{C}$  NMR (100 MHz,  $\text{CDCl}_3$ ):  $\delta$  146.80, 134.13, 128.38, 127.74, 127.10, 85.27, 50.36, 29.78, 28.49, 27.48. MS (ESI):  $[\text{M} + \text{H}]^+ = 291$ ;  $[\alpha]_{\text{D}}^{20} = -32^\circ$  ( $c = 0.0104$  g/100 mL, chloroform).

*1,1-Diphenyl-7-(1-phenyl-ethyl)-hexahydro-oxazolo[3,4-a]pyrazin-3-one (8 and 8a)*. To a stirred solution of **7** (380 mg, 1.31 mmol) in anhydrous THF (5 mL), TMEDA (0.53 mL, 3.54 mmol) was added. The reaction was cooled at  $-78^\circ\text{C}$ , and *sec*-BuLi 1.4 M in hexane (2.53 mL, 3.54 mmol) was added. The reaction was heated at  $-35^\circ\text{C}$ , and after 2 h, a solution of benzophenone (480 mg, 2.62 mmol) in anhydrous THF (7 mL) was added dropwise. The reaction became green and was stirred at room temperature for 24 h. After this time, the reaction was monitored by TLC (EtOAc/light petroleum 1:2) and quenched by adding  $\text{NH}_4\text{Cl}$  saturated solution (20 mL). The solvent was removed in vacuo and the aqueous phase extracted three times with EtOAc (30 mL). The combined organic layer was dried and evaporated to dryness. The crude diastereomers mixture was purified by flash chromatography using EtOAc/light petroleum 1:2 as eluent to obtain the fast running diastereomer **8a** in 40% yield and the low running diastereomer **8** in 45% yield.

**8a**:  $^1\text{H}$  NMR (400 MHz,  $\text{CDCl}_3$ ):  $\delta$  7.55–7.49 (m, 2H), 7.41–7.21 (m, 11H), 7.19–7.14 (m, 2H), 4.51 (dd, 1H,  $J = 10.9$ , 3.6 Hz), 3.74 (ddd, 1H,  $J = 13.2$ , 3.5, 1.3 Hz), 3.34 (q, 1H,  $J = 6.7$  Hz), 3.04 (ddd, 1H,  $J = 13.0$ , 12.1, 3.6 Hz), 2.70–2.61 (m, 2H), 1.86 (td, 1H,  $J = 11.9$ , 3.6 Hz), 1.50–1.41 (m, 1H), 1.22 (d, 3H,  $J = 6.7$  Hz).  $^{13}\text{C}$  NMR (100 MHz,  $\text{CDCl}_3$ ):  $\delta$  156.17, 142.85, 142.52, 138.91, 128.69, 128.58, 128.50, 128.35, 128.01, 127.51, 127.37, 126.19, 125.95, 85.50, 64.52, 61.56, 52.66, 49.30, 42.07, 19.34. MS ESI  $[\text{M} + \text{H}]^+ = 399$ ;  $[\alpha]_{\text{D}}^{20} = +216$  ( $c = 0.108$  g/100 mL, chloroform).

**8**:  $^1\text{H}$  NMR (400 MHz,  $\text{CDCl}_3$ ):  $\delta$  7.50–7.45 (m, 2H), 7.39–7.20 (m, 11H), 7.18–7.14 (m, 2H), 4.44 (dd, 1H,  $J = 3.56$ , 10.93 Hz), 3.86–3.79 (m, 1H), 3.48 (q, 1H,  $J = 6.8$  Hz), 3.11 (ddd, 1H,  $J = 13.0$ , 12.0, 3.81 Hz), 2.80–2.73 (m, 1H), 2.44 (ddd, 1H,  $J = 11.5$ , 3.5, 1.6 Hz), 2.07–1.97 (m, 1H), 1.50 (m, 1H), 1.27 (d, 3H,  $J = 6.8$  Hz).  $^{13}\text{C}$  NMR (100 MHz,  $\text{CDCl}_3$ ):  $\delta$  156.20, 142.48, 142.28, 138.81, 128.65, 128.51, 128.32, 127.98, 127.59, 127.28, 126.11, 125.92, 125.84, 85.39, 63.86, 61.67, 53.24, 47.58, 42.11, 17.16; MS ESI  $[\text{M} + \text{H}]^+ = 399$ ;  $[\alpha]_{\text{D}}^{20} = -132^\circ$  ( $c = 0.11$  g/100 mL, chloroform).

*3-Oxo-1,1-diphenyl-tetrahydro-oxazolo[3,4-a]pyrazine-7-carboxylic Acid 9H-fluoren-9-ylmethyl Ester (9 and 9a)*. To a stirred solution of **8** or **8a** (200 mg, 0.52 mmol) in acetonitrile (10 mL) at reflux, Fmoc-Cl (148 mg, 0.57 mmol) dissolved in acetonitrile (7 mL) was added. The reaction, monitored by TLC (EtOAc/light petroleum 1:2), was completed in 12 h. The desired precipitate was filtered off to obtain **9** or **9a** in about 67% yield and pure enough to be used in the next reaction.

3-Oxo-1,1-diphenyl-tetrahydro-oxazolo[3,4-a]pyrazine-7-carboxylic Acid 4-fluoro-benzylamide (**10** and **10a**). To a stirred solution of **9** (59 mg, 0.11 mmol) in anhydrous THF (15 mL), *p*-fluoro-benzylisocyanate (34.4 mg, 0.228 mmol) and DBU (19.2 mg, 0.126 mmol) were added. The reaction was monitored by TLC (EtOAc/light petroleum 1:2) and by mass spectrometry. After 24 h, the reaction was treated as for **8** and **8a**. The organic phase was dried and evaporate to dryness to give **10** in 76% yield after column chromatography using EtOAc/light petroleum 1/1 as eluent. <sup>1</sup>H NMR (400 MHz, CDCl<sub>3</sub>): δ 7.51–7.47 (m, 2H), 7.41–7.18 (m, 10H), 7.03–6.94 (m, 2H), 4.95 (t, 1H, *J* = 5.5 Hz), 4.45–4.27 (m, 3H), 4.03 (ddd, 1H, *J* = 13.5, 3.5, 1.2 Hz), 3.81 (dd, 1H, *J* = 13.1, 2.7 Hz), 3.69–3.60 (m, 1H), 3.05 (td, 1H, *J* = 12.7, 3.7 Hz), 2.93–2.82 (m, 1H), 2.14 (dd, 1H, *J* = 13.3, 11.3 Hz). <sup>13</sup>C NMR (100 MHz, CDCl<sub>3</sub>): δ 157.20, 156.11, 141.81, 138.30, 134.91, 129.48, 129.41, 129.17, 129.09, 128.82, 128.72, 128.37, 125.99, 125.85, 115.70, 115.48, 85.90, 60.55, 46.58, 44.47, 43.76, 41.37. MS ESI [*M* + *H*<sup>+</sup>] = 445.9; [α]<sub>D</sub><sup>20</sup> = +92 (*c* = 0.1 g/100 mL, MeOH).

Compound **10a** was obtained in the same manner, starting from **9a**. Analytical data: yield 83%. <sup>1</sup>H NMR (400 MHz, CDCl<sub>3</sub>): δ 7.51–7.47 (m, 2H), 7.41–7.18 (m, 10H), 7.03–6.94 (m, 2H), 4.95 (t, 1H, *J* = 5.5 Hz), 4.45–4.27 (m, 3H), 4.03 (ddd, 1H, *J* = 13.3, 3.6, 1.3 Hz), 3.81 (dd, 1H, *J* = 13.1, 2.7 Hz), 3.69–3.60 (m, 1H), 3.05 (td, 1H, *J* = 12.7, 3.7 Hz), 2.93–2.82 (m, 1H), 2.14 (dd, 1H, *J* = 13.3, 11.3 Hz). <sup>13</sup>C NMR (100 MHz, CDCl<sub>3</sub>): δ 157.20, 156.11, 141.81, 138.30, 134.91, 129.48, 129.41, 129.17, 129.09, 128.82, 128.72, 128.37, 125.99, 125.85, 115.70, 115.48, 85.90, 60.55, 46.58, 44.47, 43.76, 41.37. MS ESI [*M* + *H*<sup>+</sup>] = 445.9; [α]<sub>D</sub><sup>20</sup> = –91 (*c* = 0.12 g/100 mL, MeOH).

**Chiral Chromatography Analysis.** A micro HPLC (Agilent 1100 micro series, Agilent Technologies) equipped with a micro diode array detector was employed. A 150 mm × 2 mm stainless steel column packed with Lux Cellulose-1 (cellulose tris 3,5-dimethylphenylcarbamate from Phenomenex) was used for all the measurements. The average size of the packing material was 3 μm. The mobile phase was a binary mixture of hexane/isopropyl alcohol (80/20 v/v). Flow rate was 200 μL/min. Injection volume was 3 μL. Analyte solutions were filtered with PTFE filters (0.45 μm, Supelco, Bellefonte, PA, USA) before injection. All chromatograms were recorded at 230 nm. The retention times for the first (**10a**) and second (**10**) eluted enantiomers were 6.5 and 7.9 min, respectively.

**Crystal Structure Determination of Compound 8.** The crystal data of compound **8** were collected at room temperature using a Nonius Kappa CCD diffractometer with graphite monochromated Mo Kα radiation. The data sets were corrected for Lorentz and polarization effects. The structure was solved by direct methods<sup>18</sup> and refined using full-matrix least-squares with all non-hydrogen atoms anisotropically and hydrogens included on calculated positions riding on their carrier atoms. All calculations were performed using SHELXL-97<sup>19</sup> and PARST<sup>20</sup> implemented in WINGX<sup>21</sup> system of programs.

Crystal Data: C<sub>26</sub>H<sub>26</sub>N<sub>2</sub>O<sub>2</sub>, orthorhombic, space group P2<sub>1</sub>2<sub>1</sub>2<sub>1</sub>, *a* = 11.2339(2), *b* = 11.6808(3), *c* = 16.4783(5) Å, *V* = 2162.30(9) Å<sup>3</sup>, *Z* = 4, *D*<sub>c</sub> = 1.224 g cm<sup>–3</sup>, intensity data collected with θ ≤ 26°, 4215 independent reflections measured, 3460 observed reflections [*I* > 2σ(*I*)], final *R* index = 0.0365 (observed reflections), *R*<sub>w</sub> = 0.0904 (all reflections), *S* = 1.048. The absolute configuration has not been established by anomalous dispersion effects in diffraction measurements on the crystal. The enantiomer has been assigned by reference to an unchanging chiral center in the synthetic procedure. ORTEP<sup>22</sup> view of compound **8** is shown in Figure 2.

CCDC deposition number: 810351.

**Calcium Mobilization Experiments.** HEK293 cells stably expressing the murine NPSR or the human receptor isoforms NPSRIle107 and NPSRAsn107 were generated as previously described.<sup>17</sup> HEK293<sub>mNPSR</sub> and HEK293<sub>hNPSRIle107</sub> cells were maintained in DMEM medium supplemented with 10% fetal bovine serum, 2 mM L-glutamine, and

hygromycin B (100 mg/L). HEK293<sub>hNPSRAsn107</sub> cells were maintained in DMEM medium supplemented with 10% fetal bovine serum, 2 mM glutamine, and zeocin (100 mg/L). Cells were cultured at 37 °C in 5% CO<sub>2</sub> humidified air. Cells were seeded at a density of 50000 cells/well into poly-D-lysine coated 96-well black, clear-bottom plates. The following day, the cells were incubated with medium supplemented with 2.5 mM probenecid, 3 μM of the calcium sensitive fluorescent dye Fluo-4 AM, and 0.01% pluronic acid for 30 min at 37 °C. After that time, the loading solution was aspirated and 100 μL/well of assay buffer (Hank's Balanced Salt Solution; HBSS) supplemented with 20 mM 4-(2-hydroxyethyl)-1-piperazineethanesulfonic acid (HEPES), 2.5 mM probenecid, and 500 μM Brilliant Black (Aldrich) was added. Concentrated solutions (1 mM) of NPS were made in bidistilled water and kept at –20 °C. Compounds **1**, **10**, and **10a** were dissolved DMSO at a final concentration of 10 mM, and stock solutions were kept at –20 °C until use. The successive dilutions were carried out in HBSS/HEPES (20 mM) buffer (containing 0.02% bovine serum albumin fraction V). After placing both plates (cell culture and master plate) into the fluorometric imaging plate reader FlexStation II (Molecular Devices, Sunnyvale, CA), fluorescence changes were measured. Online additions were carried out in a volume of 50 μL/well. To facilitate drug diffusion into the wells in antagonist type experiments, the present studies were performed at 37 °C and three cycles of mixing (25 μL from each well moved up and down 3 times) were performed immediately after antagonist injection to the wells. Inhibition response curves were determined against the stimulatory effect of 10 nM NPS. Compounds **1**, **10**, and **10a** were injected into the wells 24 min before adding NPS.

**Data Analysis and Terminology.** The pharmacological terminology adopted in this paper is consistent with IUPHAR recommendations. Data were expressed as mean ± SEM of at least four independent experiments made in duplicate. Maximum change in fluorescence, expressed in percent of baseline fluorescence, was used to determine agonist response. Nonlinear regression analysis using GraphPad Prism software (version 4.0) allowed logistic iterative fitting of the resultant responses and the calculation of agonist potencies and maximal effects. Agonist potencies are given as pEC<sub>50</sub> (the negative logarithm to base 10 of the molar concentration of an agonist that produces 50% of the maximal possible effect). Compounds **1**, **10**, and compound **10a** antagonist properties were evaluated in inhibition response curve experiments; the antagonist potency, expressed as pK<sub>B</sub>, was derived from the following equation:

$$K_B = IC_{50} / ([2 + ([A]/EC_{50})^n]^{1/n} - 1)$$

where IC<sub>50</sub> is the concentration of antagonist that produces 50% inhibition of the agonist response, [A] is the concentration of agonist, EC<sub>50</sub> is the concentration of agonist producing a 50% maximal response, and *n* is the Hill coefficient of the concentration response curve to the agonist.

## ■ ASSOCIATED CONTENT

Supporting Information. Monodimensional and bidimensional NMR spectra of compounds **8**, **8a**, and final products and crystal data of compound **8** (CIF). This material is available free of charge via the Internet at <http://pubs.acs.org>.

## ■ AUTHOR INFORMATION

### Corresponding Author

\*Phone: +39-0532-455-988. Fax: +39-0532-455953. E-mail: r.guerrini@unife.it.

### Author Contributions

<sup>#</sup>These authors contributed equally to this work.

## ACKNOWLEDGMENT

We are grateful to Dr. Alberto Casolari and Dr. Elisa Durini for the NMR analysis and Professor Vinicio Zanirato for the helpful discussion about NMR spectra of compound **8**. This work was supported by funds from the University of Ferrara (FAR grants to G.C. and S.S.), the Italian Ministry of the University (PRIN grant to G.C. and S.S. and CHEM-PROFARMA-NET grant to A.C.), the Compagnia di S. Paolo Foundation (NPSNP grant to G.C.), and the National Institute of Mental Health (MH-71313 grant to R.K.R.).

## ABBREVIATIONS USED

DBU, 1,8-Diazabicyclo[5.4.0]undec-7-ene; DMEM, Dulbecco's Modified Eagle's Medium; DMF, *N,N*-dimethylformamide; Fmoc-Cl, 9-fluorenylmethyl chloroformate; HBSS, Hank's Balanced Salt Solution; HEK, human embryonic kidney; HEPES, 4-(2-hydroxyethyl)-1-piperazineethanesulfonic acid; MS-ESI, electron spray ionization mass spectrometry; NMDA, *N*-methyl-D-aspartic acid; PFTE, polytetrafluoroethylene; RP-HPLC, reversed-phase high-performance liquid chromatography; THF, tetrahydrofuran; TMEDA, tetramethylethylenediamine; WSC, 1-ethyl-3-(3'-dimethylaminopropyl)carbodiimide

## REFERENCES

- (1) Xu, Y. L.; Reinscheid, R. K.; Huitron-Resendiz, S.; Clark, S. D.; Wang, Z.; Lin, S. H.; Brucher, F. A.; Zeng, J.; Ly, N. K.; Henriksen, S. J.; de Lecea, L.; Civelli, O. Neuropeptide S: a neuropeptide promoting arousal and anxiolytic-like effects. *Neuron* **2004**, *43*, 487–497.
- (2) Xu, Y. L.; Gall, C. M.; Jackson, V. R.; Civelli, O.; Reinscheid, R. K. Distribution of neuropeptide S receptor mRNA and neurochemical characteristics of neuropeptide S-expressing neurons in the rat brain. *J. Comp. Neurol.* **2007**, *500*, 84–102.
- (3) Guerrini, R.; Salvadori, S.; Rizzi, A.; Regoli, D.; Calo, G. Neurobiology, pharmacology, and medicinal chemistry of neuropeptide S and its receptor. *Med. Res. Rev.* **2010**, *30*, 751–777.
- (4) Camarda, V.; Rizzi, A.; Ruzza, C.; Zucchini, S.; Marzola, G.; Marzola, E.; Guerrini, R.; Salvadori, S.; Reinscheid, R. K.; Regoli, D.; Calo, G. In vitro and in vivo pharmacological characterization of the neuropeptide s receptor antagonist [D-Cys(tBu)S]neuropeptide S. *J. Pharmacol. Exp. Ther.* **2009**, *328*, 549–555.
- (5) Guerrini, R.; Camarda, V.; Trapella, C.; Calo, G.; Rizzi, A.; Ruzza, C.; Fiorini, S.; Marzola, E.; Reinscheid, R. K.; Regoli, D.; Salvadori, S. Synthesis and biological activity of human neuropeptide S analogues modified in position 5: identification of potent and pure neuropeptide S receptor antagonists. *J. Med. Chem.* **2009**, *52*, 524–529.
- (6) Guerrini, R.; Camarda, V.; Trapella, C.; Calo, G.; Rizzi, A.; Ruzza, C.; Fiorini, S.; Marzola, E.; Reinscheid, R. K.; Regoli, D.; Salvadori, S. Further studies at neuropeptide s position 5: discovery of novel neuropeptide S receptor antagonists. *J. Med. Chem.* **2009**, *52*, 4068–4071.
- (7) Fukatsu, K.; Nakayama, Y.; Tarui, N.; Mori, M.; Matsumoto, H.; Kurasawa, O.; Banno, H. Bicyclic piperazine compound and use thereof. PCT Int. Appl. WO2005021555, 2005.
- (8) Okamura, N.; Habay, S. A.; Zeng, J.; Chamberlin, A. R.; Reinscheid, R. K. Synthesis and pharmacological in vitro and in vivo profile of 3-oxo-1,1-diphenyl-tetrahydro-oxazolo[3,4-*a*]pyrazine-7-carboxylic acid 4-fluoro-benzylamide (SHA 68), a selective antagonist of the neuropeptide S receptor. *J. Pharmacol. Exp. Ther.* **2008**, *325*, 893–901.
- (9) Ruzza, C.; Rizzi, A.; Trapella, C.; Pela, M.; Camarda, V.; Ruggieri, V.; Filaferrero, M.; Cifani, C.; Reinscheid, R. K.; Vitale, G.; Ciccocioppo, R.; Salvadori, S.; Guerrini, R.; Calo, G. Further studies on the pharmacological profile of the neuropeptide S receptor antagonist SHA 68. *Peptides* **2010**, *31*, 915–925.

- (10) Okamura, N.; Reinscheid, R. K.; Ohgake, S.; Iyo, M.; Hashimoto, K. Neuropeptide S attenuates neuropathological, neurochemical and behavioral changes induced by the NMDA receptor antagonist MK-801. *Neuropharmacology* **2010**, *58*, 166–172.

- (11) Kallupi, M.; Cannella, N.; Economidou, D.; Ubaldi, M.; Ruggieri, B.; Weiss, F.; Massi, M.; Marugan, J.; Heilig, M.; Bonnavion, P.; de Lecea, L.; Ciccocioppo, R. Neuropeptide S facilitates cue-induced relapse to cocaine seeking through activation of the hypothalamic hypocretin system. *Proc. Natl. Acad. Sci. U.S.A.* **2010**, *107*, 19567–19572.

- (12) Dal Ben, D.; Antonini, I.; Buccioni, M.; Lambertucci, C.; Marucci, G.; Vittori, S.; Volpini, R.; Cristalli, G. Molecular modeling studies on the human neuropeptide S receptor and its antagonists. *ChemMedChem* **2010**, *5*, 371–383.

- (13) Melamed, J. Y.; Zartman, A. E.; Kett, N. R.; Gotter, A. L.; Uebele, V. N.; Reiss, D. R.; Condra, C. L.; Fandozzi, C.; Lubbers, L. S.; Rowe, B. A.; McGaughey, G. B.; Henault, M.; Stocco, R.; Renger, J. J.; Hartman, G. D.; Bilodeau, M. T.; Trotter, B. W. Synthesis and evaluation of a new series of Neuropeptide S receptor antagonists. *Bioorg. Med. Chem. Lett.* **2010**, *20*, 4700–4703.

- (14) Trotter, B. W.; Nanda, K. K.; Manley, P. J.; Uebele, V. N.; Condra, C. L.; Gotter, A. L.; Menzel, K.; Henault, M.; Stocco, R.; Renger, J. J.; Hartman, G. D.; Bilodeau, M. T. Tricyclic imidazole antagonists of the Neuropeptide S Receptor. *Bioorg. Med. Chem. Lett.* **2010**, *20*, 4704–4708.

- (15) Juaristi, E.; Leon-Romo, J. L.; Reyes, A.; Escalante, J. Recent applications of alpha-phenylethylamine (alpha-PEA) in the preparation of enantiopure compounds. Part 3: alpha-PEA as chiral auxiliary. Part 4: alpha-PEA as chiral reagent in the stereodifferentiation of prochiral substrates. *Tetrahedron: Asymmetry* **1999**, *10*, 2441–2495.

- (16) Guizzetti, S.; Benaglia, M.; Rossi, S. Highly stereoselective metal-free catalytic reduction of imines: an easy entry to enantiomerically pure amines and natural and unnatural alpha-amino esters. *Org. Lett.* **2009**, *11*, 2928–2931.

- (17) Reinscheid, R. K.; Xu, Y. L.; Okamura, N.; Zeng, J.; Chung, S.; Pai, R.; Wang, Z.; Civelli, O. Pharmacological Characterization of Human and Murine Neuropeptide S Receptor Variants. *J. Pharmacol. Exp. Ther.* **2005**, *315*, 1338–1345.

- (18) Altomare, A.; Burla, M. C.; Camalli, M.; Cascarano, G. L.; Giacovazzo, C.; Guagliardi, A.; Moliterni, A. G.; Polidori, G.; Spagna, R. SIR97: a new tool for crystal structure determination and refinement. *J. Appl. Crystallogr.* **1999**, *32*, 115–119.

- (19) Sheldrick, G. M. Program for the crystal structure refinement. University of Gottingen: Gottingen, Germany, 1997; <http://shelx.uni-ac.gwdg.de/SHELX/>.

- (20) Nardelli, M. PARST95—an update to PARST: a system of Fortran routines for calculating molecular structure parameters from the results of crystal structure analyses. *J. Appl. Crystallogr.* **1995**, *28*, 659.

- (21) Farrugia, L. J. WinGX suite for small-molecule single crystal crystallography. *J. Appl. Crystallogr.* **1999**, *32*, 837–838.

- (22) Farrugia, L. J. ORTEP-3 for Windows—a version of ORTEP-III with a Graphical User Interface (GUI). *J. Appl. Crystallogr.* **1997**, *30*, 565.